

REDUCING TWO-WAY RANGING VARIANCE BY SIGNAL-TIMING OPTIMIZATION

Mohammed Ayman Shalaby*, Charles Champagne Cossette*, James Richard Forbes*, Jerome Le Ny†

* Department of Mechanical Engineering, McGill University, Montreal, QC, Canada

† Department of Electrical Engineering, Polytechnique Montreal, Montreal, QC, Canada

ABSTRACT

Time-of-flight-based range measurements among transceivers with different clocks requires ranging protocols that accommodate for the varying rates of the clocks. Double-sided two-way ranging (DS-TWR) has recently been widely adopted as a standard protocol due to its accuracy; however, the precision of DS-TWR has not been clearly addressed. In this paper, an analytical model of the variance of DS-TWR is derived as a function of the user-programmed response delays. Consequently, this allows formulating an optimization problem over the response delays in order to maximize the information gained from range measurements by addressing the effect of varying the response delays on the precision and frequency of the measurements. The derived analytical variance model and proposed optimization formulation are validated experimentally with 2 ranging UWB transceivers, where 29 million range measurements are collected.

Index Terms— two-way ranging, precision, uncertainty modelling, timing optimization

1. INTRODUCTION

A common requirement for real-time localization systems (RTLS) is a source of distance or *range* measurements between different bodies, which motivated the adoption of the IEEE 802.15.4a standard [1]. Range measurements are obtained by measuring the time-of-flight (ToF) of signals between two transceivers, which requires accurate timestamping of transmission and reception of signals at either transceiver. This problem is complicated by the transceivers' clocks running at different rates, thus introducing a time-varying offset between the clocks [2, 3]. The rate of change of this clock offset is hereinafter referred to as the *clock skew*.

The clock offsets and skews between different transceivers introduce biases in the range measurements [4, 5, 6], which are addressed by the ranging protocols presented in the IEEE 802.15.4z standard [7]. A commonly used protocol is *two-way ranging* (TWR), which relies on averaging out two ToF measurements in order to negate the effect of the clock offset. This is widely adopted in ultra-wideband (UWB)-based ranging [6, 8, 9], and is also used in underwater applications

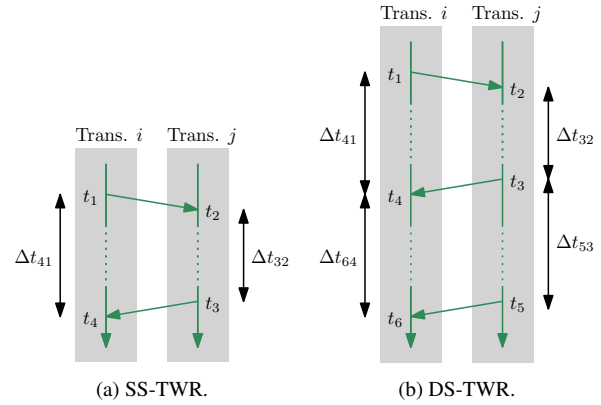


Fig. 1: Timeline schematics for two transceivers i and j showing the different TWR ranging protocols, where t_ℓ denotes the ℓ^{th} timestamp for a TWR instance and $\Delta t_{\ell k} \triangleq t_\ell - t_k$.

utilizing acoustic position systems [10], distance measuring equipment (DME) in aviation navigation [11], and other radio signals such as Zigbee [12].

This paper focuses on two variants of the TWR protocol, particularly the single-sided TWR (SS-TWR) and the double-sided TWR (DS-TWR) protocols presented in [6], both shown in Figure 1. Despite requiring an additional message transmission, the main motivation behind DS-TWR as compared to SS-TWR is to correct the clock-skew-dependent bias, which improves the accuracy of the measurements [5, 6]. Nonetheless, the *precision* of DS-TWR measurements as compared to SS-TWR measurements is a less commonly-addressed topic, where precision is typically measured by the variance of the range measurements. The variance of DS-TWR measurements has only been derived analytically as an approximate function of the true range [13] or experimentally for some fixed timing intervals [14].

The main focus of this paper is to extend the comparison between SS-TWR and DS-TWR measurements to include the variance, which allows optimizing signal timing in DS-TWR to improve precision. The contributions of this paper are summarized as follows.

- Deriving an analytical model of the variance of SS-TWR and DS-TWR that is a function of the timing of message transmissions.
- Formulating an optimization problem for DS-TWR that is a function of the signal timings in order to maximize the information collected in one unit of time.

This work was supported by the NSERC Alliance Grant program, the NSERC Discovery Grant program, the CFI JELF program, and the FRQNT.

Corresponding Author: mohammed.shalaby@mail.mcgill.ca

- Analyzing the effect of relative motion during ranging for DS-TWR
- Validating experimentally the analytical model and the optimization procedure using static UWB transceivers.

The remainder of this paper is organized as follows. The analytical model of the variance of TWR measurements is derived in Section 2, and the timing-optimization problem is formulated in Section 3. Experimental validation is then summarized in Section 4.

2. DS-TWR VARIANCE

A ToF estimate \hat{t}_f of the true ToF t_f can be computed from the SS-TWR protocol shown in Figure 1a as

$$\hat{t}_f^{ss} = \frac{1}{2}(\Delta t_{41} - \Delta t_{32}),$$

while [6] proposes a ToF estimate of the form

$$\hat{t}_f^{ds} = \frac{1}{2} \left(\Delta t_{41} - \frac{\Delta t_{64}}{\Delta t_{53}} \Delta t_{32} \right)$$

for the DS-TWR protocol shown in Figure 1b. In the presence of clock skew γ and timestamping noise η , the computed ToF error $e = \hat{t}_f - t_f$ is shown in [6] to be of the form

$$e^{ss} = \frac{1}{2} (\gamma_i \Delta t_{41} + (1 + \gamma_i) \eta_{41} - \gamma_j \Delta t_{32} - (1 + \gamma_j) \eta_{32}), \quad (1)$$

for SS-TWR, and approximately of the form

$$e^{ds} \approx \gamma_i t_f + \frac{1}{2} (1 + \gamma_i) \left[\frac{\Delta t_{32}}{\Delta t_{53}} (\eta_{53} - \eta_{64}) + \eta_{41} - \eta_{32} \right] \quad (2)$$

for DS-TWR, where γ_i is the skew of Transceiver i 's clock relative to real time, $\eta_{k\ell} = \eta_k - \eta_\ell$, and $\eta_k, \eta_\ell \sim \mathcal{N}(0, R)$ are mutually-independent timestamping white noise associated with timestamps t_k and t_ℓ , respectively.

The main motive behind using DS-TWR protocols rather than SS-TWR protocols is to correct the clock-skew-dependent bias, which can be shown by looking at the expected value of the error [5, 6]. The expected value of e^{ss} is of the form

$$\mathbb{E}[e^{ss}] = \gamma_i t_f + \frac{1}{2} (\gamma_i - \gamma_j) \Delta t_{32}, \quad (3)$$

while the expected value of e^{ds} is

$$\mathbb{E}[e^{ds}] = \gamma_i t_f, \quad (4)$$

which significantly reduces the clock-skew-dependent bias since $\Delta t_{32} \gg t_f$ for short range measurements.

Having addressed the accuracy of the measurements for SS-TWR and DS-TWR, it might appear that DS-TWR should always be used. However, the choice of ranging protocol

should also incorporate knowledge of the precision of the measurements, which has not been exclusively addressed in the literature. Revisiting (1) and (3), the variance of the SS-TWR measurements can be derived to be

$$\begin{aligned} & \mathbb{E}[(e^{ss} - \mathbb{E}[e^{ss}])^2] \\ &= \mathbb{E} \left[\left(\frac{1}{2} ((1 + \gamma_1) \eta_{41} - (1 + \gamma_2) \eta_{32}) \right)^2 \right] \\ &= \frac{1}{2} ((1 + \gamma_1)^2 + (1 + \gamma_2)^2) R. \end{aligned}$$

Similarly, by revisiting (2) and (4), the variance of the DS-TWR measurements is

$$\begin{aligned} & \mathbb{E}[(e^{ds} - \mathbb{E}[e^{ds}])^2] \\ &= \mathbb{E} \left[\left(\frac{1}{2} (1 + \gamma_1) \left(\frac{\Delta t_{32}}{\Delta t_{53}} (\eta_{53} - \eta_{64}) + \eta_{41} - \eta_{32} \right) \right)^2 \right] \\ &= (1 + \gamma_1)^2 \left(1 + \frac{\Delta t_{32}}{\Delta t_{53}} + \frac{(\Delta t_{32})^2}{(\Delta t_{53})^2} \right) R. \end{aligned} \quad (5)$$

Therefore, in the absence of clock skew (i.e., when $\gamma_1 = \gamma_2 = 0$, often assumed since $\gamma_1, \gamma_2 \ll 1$), the variance of DS-TWR measurements is typically greater than SS-TWR measurements, and approaches the variance of SS-TWR as $\Delta t_{32} \rightarrow 0$ and/or $\Delta t_{53} \rightarrow \infty$. The $\Delta t_{32} \rightarrow 0$ condition is due to the effect of the length of Δt_{32} on the bias, and the $\Delta t_{53} \rightarrow \infty$ condition is due to the fact that the ratio $\frac{\Delta t_{64}}{\Delta t_{53}}$ is being used to obtain a clock-skew measurement, and the longer the Δt_{53} interval is the greater the signal-to-timestamping-noise ratio.

3. DS-TWR TIMING OPTIMIZATION

The timing delays Δt_{32} and Δt_{53} affect the variance of the measurements, the frequency of the measurements, and the ranging error due to relative motion between the transceivers. In Section 3.1, the choice of delays is motivated as a function of the variance and frequency of the measurements while assuming no relative motion between the transceivers. This assumption is then validated in Section 3.2 for the utilized DS-TWR protocol, showing that motion can indeed be neglected when choosing the timing delays.

3.1. Finding Optimal Timing Delays

Given (5), minimizing Δt_{32} within the limitations of the system is an obvious choice to reduce the measurement variance. However, it is less clear what is the right choice with Δt_{53} , as maximizing this second-response delay reduces measurement uncertainty but also reduces the frequency of measurements. The choice of Δt_{53} is thus application-specific. Most commonly in estimation applications, the goal is to minimize the uncertainty of the estimates, which is achieved by maximizing the *information* attained from measurements. There-

fore, this section poses an information-maximizing (variance-minimizing) optimization problem.

The amount of information obtained in one unit of time is a function of the uncertainty of the individual measurement and the number of measurements in that unit of time. As a result, the *optimal* delay is one that is long enough to reduce the uncertainty of the individual measurement but short enough to ensure measurements are recorded at a sufficient frequency.

Revisiting (5), the uncertainty of the individual measurement can be rewritten in the absence of clock skews since $\gamma_i \ll 1$, yielding

$$R_{\text{meas}} \triangleq R + \frac{\Delta t_{32}}{\Delta t_{53}} R + \left(\frac{\Delta t_{32}}{\Delta t_{53}} \right)^2 R.$$

Meanwhile, the frequency of the measurements is dependent on $\Delta t_{32} + \Delta t_{53}$ as well as any further processing to retrieve the range measurements, such as reading the raw timestamps from the registers and computing the range measurement from the raw timestamps. The time taken for computational processing is defined as T , which is assumed to be constant for the same experimental set-up. Therefore, the time-length of one measurement is $T + \Delta t_{32} + \Delta t_{53}$ seconds long. The delay Δt_{32} is to be minimized as much as the hardware allows, and Δt_{53} is to be optimized as follows. In one second, a total of $\left[\frac{1}{T + \Delta t_{32} + \Delta t_{53}} \right]$ measurements occur, meaning that the overall uncertainty of the measurements (or the inverse of accumulated information in one second) is given as

$$R_{\text{tot}}(\Delta t_{53}) \triangleq [T + \Delta t_{32} + \Delta t_{53}] R_{\text{meas}}(\Delta t_{53}). \quad (6)$$

Finding the optimal delay Δt_{53}^* is then found by solving

$$\Delta t_{53}^* = \arg \min_{\Delta t_{53} \in \mathbb{R}} R_{\text{tot}}(\Delta t_{53}). \quad (7)$$

The derivative of (6) w.r.t. Δt_{53} is

$$\begin{aligned} \frac{dR_{\text{tot}}}{d\Delta t_{53}} &= R - (T + \Delta t_{32}) \frac{\Delta t_{32}}{(\Delta t_{53})^2} R \\ &\quad - 2(T + \Delta t_{32}) \frac{(\Delta t_{32})^2}{(\Delta t_{53})^3} R - \frac{(\Delta t_{32})^2}{(\Delta t_{53})^2} R, \end{aligned}$$

and equating to 0 yields the cubic polynomial

$$0 = (\Delta t_{53})^3 - \Delta t_{32}(T + 2\Delta t_{32})\Delta t_{53} - 2(\Delta t_{32})^2(T + \Delta t_{32}). \quad (8)$$

The value for T and the minimum value of Δt_{32} can be determined experimentally and are both processor and application dependent. As an example where $T = 7.2$ ms and $\Delta t_{32} = 0.35$ ms, the optimal delay can be found analytically to be approximately 1.9 ms using (8). The overall uncertainty R_{tot} as a function of Δt_{53} for $T = 7.2$ ms at different values of Δt_{32} is shown in Figure 2.

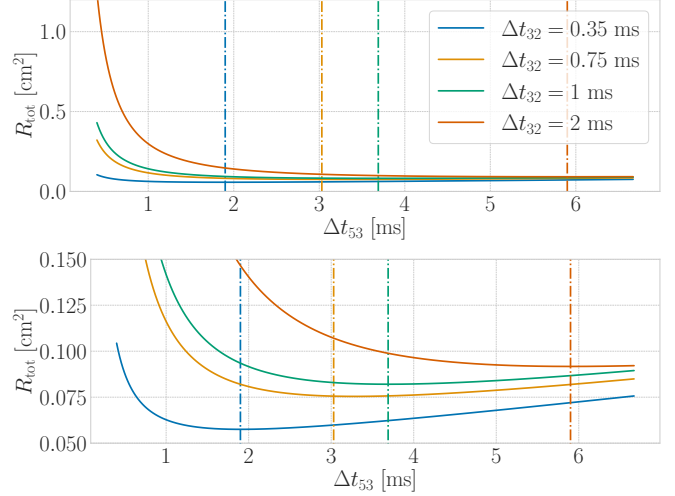


Fig. 2: The theoretical overall uncertainty R_{tot} as a function of the delay Δt_{53} for 4 different values of Δt_{32} . All curves use $T = 7.2$ ms, which is experimentally determined for the set-up used in Section 4. The vertical dotted lines correspond to the analytically-evaluated minimum of the colour-matched plotted curves. The bottom plot is a close-up view of the top plot.

3.2. Relative Motion During Ranging

Commonly, a constant distance throughout ranging is assumed, but this assumption holds less the longer the response delay. To address this, assume the less-restrictive case of no relative acceleration between the transceivers. In this case, the three ToF measurements shown in Figure 1b are of different distances, and are related by

$$t_f^2 = t_f^1 + \bar{v}\Delta t_{32}, \quad t_f^3 = t_f^2 + \bar{v}\Delta t_{53},$$

where $\bar{v} = v/c$, v is the rate of change of the distance between transceivers, and c is the speed of light. Note that motion during the intervals Δt_{32} and Δt_{53} is addressed since the intervals are in the order of milliseconds. Meanwhile, ToF is in the order of nanoseconds for short range measurements, and motion in between time of transmission and reception is therefore negligible for most applications.

The computed ToF measurement using the DS-TWR protocol is then

$$\begin{aligned} \hat{t}_f^{\text{ds}} &= \frac{1}{2} \left(\Delta t_{41} - \frac{\Delta t_{64}}{\Delta t_{53}} \Delta t_{32} \right) \\ &= \frac{1}{2} \left(t_3 + t_f^2 - t_1 \right. \\ &\quad \left. - \frac{t_5 + t_f^3 - t_3 - t_f^2}{\Delta t_{53}} (t_2 + \Delta t_{32} - t_1 - t_f^1) \right) \\ &= \frac{1}{2} \left(t_2 + \Delta t_{32} + t_f^1 \right. \\ &\quad \left. + \bar{v}\Delta t_{32} - t_1 - \frac{\Delta t_{53} + \bar{v}\Delta t_{53}}{\Delta t_{53}} \Delta t_{32} \right) \\ &= t_f^1, \end{aligned}$$

meaning that the computed ToF corresponds to the distance between the transceivers at the beginning of ranging, and the



Fig. 3: The experimental set-up. (Left) Custom-built circuit board, using the DWM1000 UWB transceiver. (Right) Two static tripods placed 1.5 metres apart, each holding a UWB transceiver.

error due to motion is independent from the delays Δt_{32} and Δt_{53} . Therefore, a particular feature of the DS-TWR protocol presented in [6] is that the timing optimization can be done without addressing errors due to motion. A similar analysis on the DS-TWR protocol proposed in [5] shows that the error in the ranging measurements due to motion is a complicated function of the velocity and the delays.

4. EXPERIMENTAL EVALUATION

To evaluate the effect of the second-response delay Δt_{53} on a real system, the following experiment is performed. Two custom-made circuit boards equipped with DWM1000 UWB transceivers [15] are fixed to two static tripods as shown in Figure 3. They are both connected to a Dell XPS13 computer running Ubuntu Desktop 20.04. The second-response delay Δt_{53} is then sampled randomly many times, and for each trial 2500 measurements are collected to compute the average variance and frequency for that specific value of Δt_{53} . The results for two different values of Δt_{32} are shown in Figure 4, where $T = 7.2$ ms is found experimentally to be the amount of time required by the computer to process a range measurement. The experiment with $\Delta t_{32} = 0.35$ ms involves 5000 trials for a total of 12.5 million measurements, while the experiment with $\Delta t_{32} = 2$ ms involves 6600 trials for a total of 16.5 million measurements.

Given that this is a static experiment, R_{tot} essentially represents the uncertainty in the measurement obtained by averaging out all recorded measurements over a span of one second. Crucially, both experiments presented here match the theoretical expectations quite well. As Δt_{53} increases, both the standard deviation and the frequency of the measurements decrease, and the optimal Δt_{53} can then be found by finding the value that minimizes R_{tot} . The experimental minimum does match the theoretical minimum, thus motivating the presented analytical optimization problem (7). Lastly, as expected, the experiments with a longer Δt_{32} have an order of magnitude higher standard deviation in the measurements,

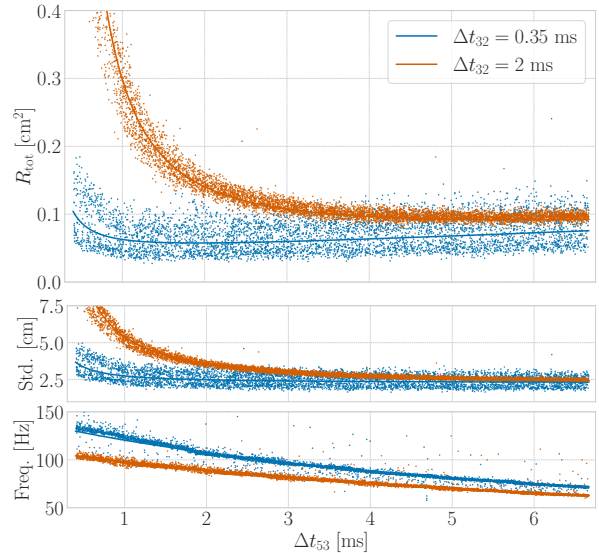


Fig. 4: The theoretical and experimental metrics as they vary with Δt_{53} . Each point corresponds to one trial of 2500 measurements, and the solid line is the theoretical curve based on the derived analytical models. The solid line matches the experimental readings. The plots show the variation of the overall uncertainty R_{tot} , the standard deviation, and the frequency of the measurements as a function of Δt_{53} for two different values of Δt_{32} .

and in both experiments the standard deviation decreases as Δt_{53} increases.

In addition to the DS-TWR experiment, a SS-TWR experiment is performed with 145 trials, for a total of 362500 measurements. Nothing varied in between trials, but the purpose of this experiment is to obtain the average standard deviation of SS-TWR experiments in order to evaluate whether the DS-TWR standard deviation does indeed converge to that of SS-TWR as $\Delta t_{53} \rightarrow \infty$ as suggested in Section 2. The SS-TWR standard deviation is found to be about 2.8 cm, while the curves in Figure 4 converge to a standard deviation of approximately 2.5 cm. The slightly higher SS-TWR variance is due to the effect of clock skew, as the SS-TWR measurements drift over the 2500 range measurements of a single trial, which increases the computed standard deviation.

5. CONCLUSION

This paper extends the comparison of SS-TWR and DS-TWR to include precision by deriving an analytical model of the variance as a function of the signal timings of the ranging protocols. This consequently allows optimizing over the timing delays in order to minimize the variance of DS-TWR measurements, and an optimization problem is then formulated to maximize information by balancing the effect of reduced variance and reduced frequency of measurements as timing delays increase. It is also shown that the effect of motion is independent of the timing delays in the utilized DS-TWR protocol. Lastly, the analytical variance model and optimization procedure are evaluated on an experimental set-up with two static ranging UWB transceivers.

6. REFERENCES

[1] IEEE Computer Society, *IEEE Standard for Low-Rate Wireless Networks. Amendment 1: Add Alternate PHYs (IEEE Std 802.15.4a)*, Number 2. 2018.

[2] Alan Bensky, *Wireless Positioning Technologies and Applications*, Artech House, Inc., USA, 2007.

[3] Zafer Sahinoglu, Sinan Gezici, and Ismail Güvenc, *Ultra-wideband Positioning Systems: Theoretical Limits, Ranging Algorithms, and Protocols*, Cambridge University Press, 2008.

[4] Myungkyun Kwak and Jongwha Chong, “A new double two-way ranging algorithm for ranging system,” *Proceedings of the IEEE International Conference on Network Infrastructure and Digital Content*, pp. 470–473, 2010.

[5] Dries Neirynck, Eric Luk, and Michael McLaughlin, “An alternative double-sided two-way ranging method,” *Proceedings of the 2016 13th Workshop on Positioning, Navigation and Communication, WPNC 2016*, pp. 16–19, 2017.

[6] Mohammed Ayman Shalaby, Charles Champagne Cossette, James Richard Forbes, and Jerome Le Ny, “Calibration and Uncertainty Characterization for Ultra-Wideband Two-Way-Ranging Measurements,” *arXiv: 2210.05888*, 2022.

[7] IEEE Computer Society, *IEEE Standard for Low-Rate Wireless Networks. Amendment 1: Enhanced Ultra Wideband (UWB) Physical Layers (PHYs) and Associated Ranging Techniques (IEEE Std 802.15.4z)*, 2020.

[8] Benjamin Hepp, Tobias Nägeli, and Otmar Hilliges, “Omni-directional person tracking on a flying robot using occlusion-robust ultra-wideband signals,” *IEEE International Conference on Intelligent Robots and Systems*, vol. 2016-Novem, pp. 189–194, 2016.

[9] Taavi Laadung, Sander Ulp, Muhammad Mahtab Alam, and Yannick Le Moullec, “Novel Active-Passive Two-Way Ranging Protocols for UWB Positioning Systems,” *IEEE Sensors Journal*, vol. 22, no. 6, pp. 5223–5237, 2022.

[10] Keith Vickery, “Acoustic positioning systems - a practical overview of current systems,” *Proceedings of the IEEE Symposium on Autonomous Underwater Vehicle Technology*, pp. 5–17, 1998.

[11] Sherman Lo, Yu Hsuan Chen, Per Enge, Robert Erikson, and Robert Lilley, “Distance measuring equipment accuracy performance today and for future alternative position navigation and timing (APNT),” *26th International Technical Meeting of the Satellite Division of the Institute of Navigation, ION GNSS 2013*, vol. 1, pp. 711–721, 2013.

[12] Bhola Raj Panta, Kohta Kido, Satoshi Yasuda, Yuko Hanado, Seiji Kawamura, Hiroshi Hanado, Kenichi Takizawa, Masugi Inoue, and Nobuyasu Shiga, “Distance variation monitoring with wireless two-way interferometry (Wi-WI),” *Sensors and Materials*, vol. 31, no. 7, pp. 2313–2321, 2019.

[13] Václav Navrátil and František Vejražka, “Bias and variance of asymmetric double-sided two-way ranging,” *Navigation, Journal of the Institute of Navigation*, vol. 66, no. 3, pp. 593–602, 2019.

[14] Cung Lian Sang, Michael Adams, Timm Hörmann, Marc Hesse, Mario Porrmann, and Ulrich Rückert, “Numerical and experimental evaluation of error estimation for two-way ranging methods,” *Sensors (Switzerland)*, vol. 19, no. 3, 2019.

[15] Qorvo, “DW1000,” <https://www.qorvo.com/products/p/DW1000>.